Inter-Layer interaction induced electronic properties in partially oxidized transition metal dichalcogenides

Soumya Ranjan Das, and Sudipta Dutta

View Online   Export Citation

Inter-Layer Interaction Induced Electronic Properties in Partially Oxidized Transition Metal Dichalcogenides

Soumya Ranjan Das[a] and Sudipta Dutta

Department of Physics, Indian Institute of Science Education and Research (IISER) Tirupati, Tirupati - 517507, Andhra Pradesh, India

[a)]Corresponding author: soumya.das@students.iisertirupati.ac.in

Abstract. We perform first-principles calculations to investigate the electronic properties of two dimensional (2D) self-assembled heterojunctions of partially oxidized mono- and bi-layer transition metal dichalcogenides (TMDs). Pristine 2D TMDs are direct band gap semiconductors. Selective oxidation leads to a broad spectrum of electronic properties, ranging from indirect band gap semiconductor to semi-metallic behavior. We tune the interlayer interaction in bilayer TMDs by selective oxidation of either top or bottom surface of the top layer with a partially oxidized bottom layer. In particular, we observe that the intrinsic inversion symmetry of the bilayer TMDs gets broken when the bottom surface of the top layer is fully oxidized. Moreover, interlayer charge transfer results in an unprecedented metallic state with completely decoupled non-degenerate bands near the Fermi energy, arising exclusively from either top or bottom layer. Our study reveals a huge possibility for these dichalcogenide based heterojunctions to be exploited in advanced optoelectronic and valleytronic device applications.

INTRODUCTION

The search for low dimensional materials beyond graphene [1-3] has spurred renewed interest on layered transition metal dichalcogenides [4], mainly due to its sizeable direct band gap that has interesting electronic, opto-electronic and valleytronic properties [5,6], and is fervently applied nowadays to develop atomically thin devices, such as FETs [7], photodetectors [8] and light emitting diodes [9].

Apart from edges or defect sites, pristine TMDs are passive due to the absence of any dangling bonds. Recent experimental and theoretical work [10,11] has shown that in the presence of ozone environment, chalcogen atoms are selectively replaced by oxygen atoms. The oxidation is temperature regulated due to the creation of an amorphous oxide composite that protects underlying layers from futher oxidation. The system becomes hole-doped due to the surface charge transfer to the oxidized layer. This gives rise to a variety of electronic properties [11] and thus such system finds important applications in FETs [12] and photogating effects [13].

In this paper, we investigate how these layer-by-layer oxidation of mono- and bi-layer TMDs can be used to tune the inter-layer interaction and its consequent effect on the electronic properties within *ab initio* calculations. We have systematically presented the results of the MoS_2 system in the following sections. However, our results are expected to be similar for any 2D semiconducting layered TMDs.

COMPUTATIONAL METHOD

For structural relaxation and for electronic property calculations, we use the first-principles method as implemented in SIESTA [14]. We perform spin-polarized calculations with anti-ferromagnetic spin orientation guess for the initial wavefunction, within generalized gradient approximation (GGA) with Perdew-Burke-Ernzerhof (PBE) exchange and correlation functional [15] and consider the double zeta polarized (DZP) basis set. The pseudopotentials have been generated within a Troullier-Martins scheme with non-relativistic electrons. An energy

cutoff of 400 Ry has been taken for the real space mesh size with a Brillouin zone sampling over a $20 \times 20 \times 1$ and $100 \times 100 \times 1$ Monkhorst-Pack grid for structural relaxation and subsequent electronic property calculations, respectively. All the structures along with their lattice vectors have been relaxed until the force on each atom reaches 0.04 eV/Å and sufficient vacuum has been created in the non-periodic z-direction.

RESULTS AND DISCUSSION

Fig. 1(a) shows the schematic picture of partially oxidized monolayer MoOS, where the bottom surface of the monolayer has been oxidized by replacing the S atoms by O atoms. Our 2D system has an underlying honeycomb lattice due to which the corresponding Brillouin zone is hexagonal. Previous phonon dispersion calculations confirm that the structure is stable [11]. Replacement of S atom by O atom from the bottom surface of monolayer MoS_2 reduces the band gap, as shown in Fig. 1(b) and Fig. 1(c), due to intra-layer charge transfer from 4d orbital of Mo to 2p orbital of O, owing to the higher electronegativity of oxygen. This also changes the dispersion of the top valence bands, whose maximum now appears at the Γ point (See Fig. 1(b)). Thus, there is a transition from direct band-gap of pristine MoS_2 to in-direct band gap of partially oxidized monolayer MoOS, resulting in the disappearance of the photoluminescence peak, as observed in previous experiments [10].
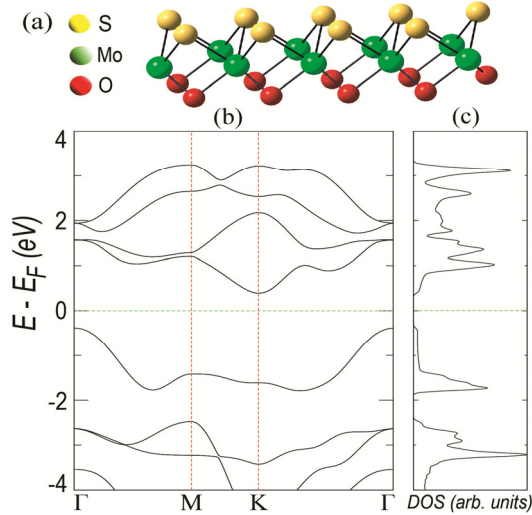

FIGURE 1. (a) The schematic representation of partially oxidized monolayer 2H-MoS_2 with trigonal prismatic geometry. In the bottom surface, all the S atoms are replaced by O atoms, to make it MoOS stoichiometry. (b) and (c) show the band structures and the corresponding density of states (DOS), respectively. The horizontal (vertical) dashed lines show the location of Fermi energy (high-symmetric points of hexagonal Brillouin zone).

Now, we want to see the effect on the electronic properties when such monolayer is vertically stacked on pristine or oxidized TMD layer to form a bilayer system. Pristine bilayer MoS_2 is an indirect band gap semiconductor. The replacement of S atoms from the bottom surface of the bottom layer reduces the indirect band gap due to intralayer charge transfer from the 4d orbital of Mo to 2p orbital of O (see Fig. 2(a1), Fig. 2(a2) and Fig. 2(a3)). However, a partially oxidized MoOSand a fully oxidized MoO_2 (see Fig. 2(b1)) shows an unprecedented semi-metallic state (see Fig. 2(b2) and Fig. 2(b3)) where the conduction band minima (at K point) and the valence band maxima (at Γ point) appear at different k-points. This system is expected to show valley polarization and can be considered as a new topological phase of charge carriers originating at the interface [11].
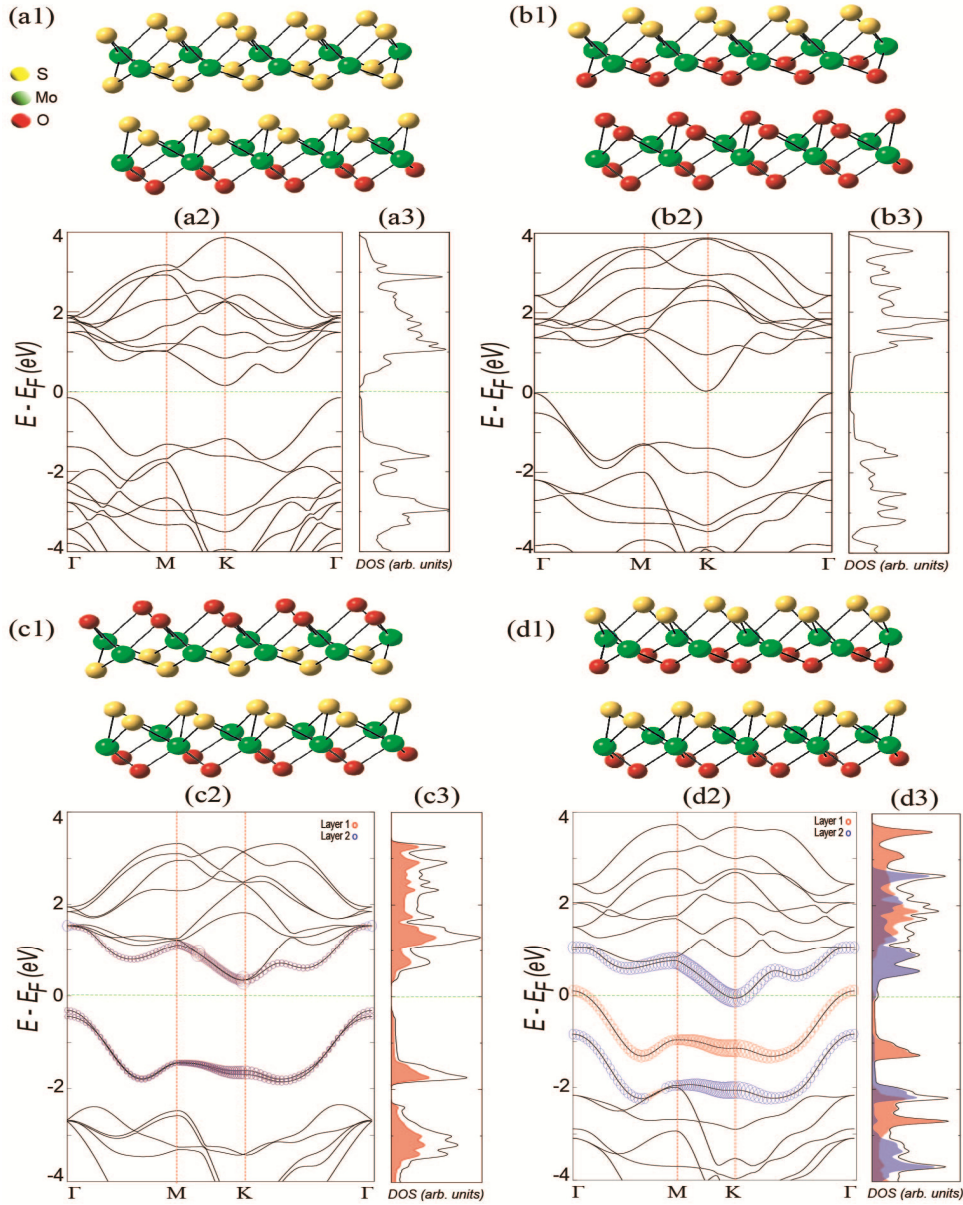
FIGURE 2. (a), (b), (c) and (d) denote the four different partially oxidized bilayer 2H-MoS$_2$ systems. Their schematic representation with the selective oxidized structure is shown in (a1), (b1), (c1) and (d1). (a2), (b2), (c2), (d2) and (a3), (b3), (c3) and (d3) denote the band structures and the corresponding DOS, respectively. Additionally, (c2), (d2) along with (c3), (d3) show the contribution of the 4d orbitals of Mo atoms and the projected DOS (pDOS) from the bottom (top) layer, respectively (denoted in orange (blue) circles and colored regions in the DOS). The size of the circles is directly proportional to the amount of contribution. The horizontal (vertical) dashed lines in the band structures and the DOS depicts the location of the Fermi energy (high symmetric points of the hexagonal Brillouin zone).

In both the bilayer systems in Fig. 2(a1) and Fig. 2(b1), the atoms at the bottom surface of the top layer and the top surface of the bottom layer are identical. In order to tune the interlayer interaction, we take the bilayer of MoOS, where the bottom surface of the top layer is either S or O atoms (see Fig. 2(c1) and Fig. 2(d1)).

From the Fig. 2(c1), it is clear that the system posses inversion symmetry. Fig. 2(c2) and Fig. 2(c3) shows that the bands near Fermi energy are degenerate and resembles the band structure of monolayer MoOS. This is due to minimal band splitting, owing to the very weak interlayer interaction.

The structure shown in Fig. 2(d1) is unique as it is intrinsically valley polarized due to the absence of an inversion center. The symmetry breaking has a clear manifestation in the band structure. Moreover, the higher electronegativity of O atom present in the bottom surface of top layer, induces interlayer charge transfer, making the system metallic as is evident from Fig. 2(d2) and Fig. 2(d3). The symmetry breaking obliterate the valley degeneracy of the bands near the Fermi energy (see Fig. 2(d2)). Hence, they are decoupled from each other and originates either from the top or the bottom layer. This is evident from the pDOS and fatband analysis shown in Fig. 2(d2) and Fig. 2(d3). This behavior induced by intrinsic symmetry breaking is quite unique in TMD systems and thus can be utilized in solar cell applications, optoelectronics and valley physics.

CONCLUSION

To summarize, we have studied the electronic properties of partially oxidized monolayer and bilayer TMD systems, MoS_2, within *ab initio* calculations. The oxidation of monolayer MoS_2 induces a direct to in-direct band gap transition. The band gap gets reduced due to intralayer charge transfer. Bilayer MoS_2 exhibit indirect gap semi-conducting properties. However the band gap reduce on partial oxidation, again due to intralayer charge transfer. A fully oxidized bottom layer with a partially oxidized top layer results in an exotic semi-metallic state. The effect of interlayer interaction is studied by taking bilayer MoOS with the bottom surface of the top layer containing either S or O atoms. The system with the O atoms at the bottom surface of top and bottom layer breaks inversion symmetry. This breaks the valley degeneracy and results in decoupling of bands near Fermi energy, localizing the top valence band and bottom conduction band on either layers. Such unique properties in TMDs, arising due to tuning of interlayer interaction, can be exploited for advance optoelectronic and valleytronic device applications.

ACKNOWLEDGMENTS

REFERENCES

1. K.S. Novoselov, D. Jiang, F. Schedin, T.J. Booth, V.V. Khotkevich, S.V. Morozov, and A.K. Geim, Proc. Nat. Acad. Sci. **102**, 10451 (2005).
2. A.K. Geim and K.S. Novoselov, Nature Mater. **6**, 183 (2007).
3. A.H.C. Neto, F. Guinea, N.M.R. Peres, K.S. Novoselov, and A.K. Geim, Rev. Mod. Phys. **81**, 109 (2009).
4. G.R. Bhimanapati et al., ACS Nano, **9**, 11509, (2015).
5. K.F. Mak, C. Lee, J. Hone, J. Shan, and T.F. Heinz, Phys. Rev. Lett. **105,** 136805 (2010).
6. M. Chhowalla, H.S. Shin, G. Eda, L.J. Li, K.P. Loh and H. Zhang, Nature Chem. **5**, 263 (2013).
7. K. Hsieh, V. Kochat, X. Zhang, Y. Gong, C.S. Tiwary, P.M. Ajayan and A. Ghosh, Nano Lett. **17**, 5452 (2017).
8. O Lopez-Sanzhez, D. Lembke, M. Kayci, A. Radenovic and A. Kis, Nature Nanotech.,**8**, 497 (2013).
9. J.S. Ross et al., Nature Nanotech.,**9**, 268, (2014).
10. M. Yamamoto, S. Dutta, S. Aikawa, S. Nakaharai and K. Wakabayashi, Nano Lett. **15**, 2067 (2015).
11. S. R. Das, K. Wakabayashi, M. Yamamoto, K. Tsukagoshi, and S. Dutta, J. Phys. Chem. C **122**, 17001 (2018).
12. M. Yamamoto, S. Nakaharai, K. Ueno and K. Tsukagoshi, Nano Lett. **16**, 2720 (2016).
13. M. Yamamoto, K. Ueno and K. Tsukagoshi, Appl. Phys. Lett. **112**, 181902 (2018).
14. J.M. Soler, E. Artacho, J.D. Gale, A. Garcia, J. Junquera, P. Ordejon, and D. Sanchez-Portal, J. Phys.: Condens. Matter **14**, 2745 (2002).
15. J.P. Perdew, K. Burke, and M. Ernzerhof, Phys. Rev. Lett. **77**, 3865 (1996).